AFRL-AFOSR-VA-TR-2017-0059

A New Paradigm for Turbulence Control for Drag Reduction

Mahmoud Hussein
REGENTS OF THE UNIVERSITY OF COLORADO THE
3100 MARINE ST 572 UCB
BOULDER, CO 80309-0001

03/10/2017
Final Report

DISTRIBUTION A: Distribution approved for public release.

Air Force Research Laboratory
AF Office Of Scientific Research (AFOSR)/RTA1

REPORT DOCUMENTATION PAGE	*Form Approved* *OMB No. 0704-0188*

1. REPORT DATE *(DD-MM-YYYY)*	**2. REPORT TYPE**	**3. DATES COVERED** *(From - To)*
02/27/2017	Final Report	Sep 30, 2015 - Sep 29, 2016

4. TITLE AND SUBTITLE

A New Paradigm for Turbulence Control for Drag Reduction

5b. GRANT NUMBER
FA9550-15-1-0495

5c. PROGRAM ELEMENT NUMBER

6. AUTHOR(S)

Professor Mahmoud Hussein

5d. PROJECT NUMBER

5e. TASK NUMBER

5f. WORK UNIT NUMBER

7. PERFORMING ORGANIZATION NAME(S) AND ADDRESS(ES)
Regents of the University of Colorado
3100 Marine Street
Boulder, CO 80303-1058

8. PERFORMING ORGANIZATION REPORT NUMBER
N/A

9. SPONSORING/MONITORING AGENCY NAME(S) AND ADDRESS(ES)
Air Force Office of Scientific Research
875 North Randolph Street
Suite 325, Room 3112
Arlington VA, 22203

10. SPONSOR/MONITOR'S ACRONYM(S)
ONR

11. SPONSOR/MONITOR'S REPORT NUMBER(S)
0414.01.0960B

12. DISTRIBUTION/AVAILABILITY STATEMENT

DISTRIBUTION A: Distribution approved for public release.

13. SUPPLEMENTARY NOTES

14. ABSTRACT

Direct numerical simulations (DNS) of spanwise-rotating turbulent channel flow as well as the neutral and unstable turbulent Ekman layer were conducted. These DNS results were used to evaluate various turbulence and heat transfer models for the Reynolds stresses, turbulent heat fluxes and higher-order moments of velocity and temperature. Explicit Algebraic Reynolds Stress Models (EARSM) obtained the Reynolds stress distributions in best agreement with DNS data for rotational flows and turbulent heat flux distributions obtained from two explicit algebraic heat flux models consistently displayed increasing disagreement with DNS data with increasing rotation rate. DNS results were also used to determine the proper computational box size for a minimal flow unit (MFU) at Ro_b=0.5. For the neutrally stratified Ekman layer, the higher-order moments of velocity were examined and the accuracy of a kurtosis model was assessed. For the unstable Ekman layer, the analysis of higher-order moments was extended to temperature-velocity correlations. These flow fields represent complex turbulence which will be subject to flow and heat transfer control by phonons at a later stage of our work. Research aimed at the control of fully turbulent channel flow using DNS was also conducted. The reduction of the kinetic energy of large amplitude perturbations in channel flow was investigated using passive phononic structures. These studies, and the results obtained, lay the foundation for extending the phononic subsurface control methodology to turbulent drag in channel flows. Results from this seed grant have appeared in three journal articles and have been accepted for presentation at national conferences

15. SUBJECT TERMS

16. SECURITY CLASSIFICATION OF:			**17. LIMITATION OF ABSTRACT**	**18. NUMBER OF PAGES**	**19a. NAME OF RESPONSIBLE PERSON**
a. REPORT	**b. ABSTRACT**	**c. THIS PAGE**			Mahmoud Hussein
					19b. TELEPHONE NUMBER *(Include area code)* 303 492 3177

DISTRIBUTION A: Distribution approved for public release.

Standard Form 298 (Rev. 8/98)
Prescribed by ANSI Std. Z39.18

INSTRUCTIONS FOR COMPLETING SF 298

1. REPORT DATE. Full publication date, including day, month, if available. Must cite at least the year and be Year 2000 compliant, e.g. 30-06-1998; xx-06-1998; xx-xx-1998.

2. REPORT TYPE. State the type of report, such as final, technical, interim, memorandum, master's thesis, progress, quarterly, research, special, group study, etc.

3. DATE COVERED. Indicate the time during which the work was performed and the report was written, e.g., Jun 1997 - Jun 1998; 1-10 Jun 1996; May - Nov 1998; Nov 1998.

4. TITLE. Enter title and subtitle with volume number and part number, if applicable. On classified documents, enter the title classification in parentheses.

5a. CONTRACT NUMBER. Enter all contract numbers as they appear in the report, e.g. F33315-86-C-5169.

5b. GRANT NUMBER. Enter all grant numbers as they appear in the report. e.g. AFOSR-82-1234.

5c. PROGRAM ELEMENT NUMBER. Enter all program element numbers as they appear in the report, e.g. 61101A.

5e. TASK NUMBER. Enter all task numbers as they appear in the report, e.g. 05; RF0330201; T4112.

5f. WORK UNIT NUMBER. Enter all work unit numbers as they appear in the report, e.g. 001; AFAPL30480105.

6. AUTHOR(S). Enter name(s) of person(s) responsible for writing the report, performing the research, or credited with the content of the report. The form of entry is the last name, first name, middle initial, and additional qualifiers separated by commas, e.g. Smith, Richard, J, Jr.

7. PERFORMING ORGANIZATION NAME(S) AND ADDRESS(ES). Self-explanatory.

8. PERFORMING ORGANIZATION REPORT NUMBER. Enter all unique alphanumeric report numbers assigned by the performing organization, e.g. BRL-1234; AFWL-TR-85-4017-Vol-21-PT-2.

9. SPONSORING/MONITORING AGENCY NAME(S) AND ADDRESS(ES). Enter the name and address of the organization(s) financially responsible for and monitoring the work.

10. SPONSOR/MONITOR'S ACRONYM(S). Enter, if available, e.g. BRL, ARDEC, NADC.

11. SPONSOR/MONITOR'S REPORT NUMBER(S). Enter report number as assigned by the sponsoring/ monitoring agency, if available, e.g. BRL-TR-829; -215.

12. DISTRIBUTION/AVAILABILITY STATEMENT. Use agency-mandated availability statements to indicate the public availability or distribution limitations of the report. If additional limitations/ restrictions or special markings are indicated, follow agency authorization procedures, e.g. RD/FRD, PROPIN, ITAR, etc. Include copyright information.

13. SUPPLEMENTARY NOTES. Enter information not included elsewhere such as: prepared in cooperation with; translation of; report supersedes; old edition number, etc.

14. ABSTRACT. A brief (approximately 200 words) factual summary of the most significant information.

15. SUBJECT TERMS. Key words or phrases identifying major concepts in the report.

16. SECURITY CLASSIFICATION. Enter security classification in accordance with security classification regulations, e.g. U, C, S, etc. If this form contains classified information, stamp classification level on the top and bottom of this page.

17. LIMITATION OF ABSTRACT. This block must be completed to assign a distribution limitation to the abstract. Enter UU (Unclassified Unlimited) or SAR (Same as Report). An entry in this block is necessary if the abstract is to be limited.

A New Paradigm for Turbulence Control for Drag Reduction

Mahmoud I. Hussein* and Sedat Biringen†

Department of Aerospace Engineering Sciences,

University of Colorado Boulder, Boulder, Colorado 80309, USA

Abstract

Direct numerical simulations (DNS) of spanwise-rotating turbulent channel flow as well as the neutral and unstable turbulent Ekman layer were conducted. These DNS results were used to evaluate various turbulence and heat transfer models for the Reynolds stresses, turbulent heat fluxes and higher-order moments of velocity and temperature. Explicit Algebraic Reynolds Stress Models (EARSM) obtained the Reynolds stress distributions in best agreement with DNS data for rotational flows and turbulent heat flux distributions obtained from two explicit algebraic heat flux models consistently displayed increasing disagreement with DNS data with increasing rotation rate. DNS results were also used to determine the proper computational box size for a minimal flow unit (MFU) at $Ro_{\mathrm{b}} = 0.5$, spanwise arrays of Taylor-Gortler vortices in the highly turbulent pressure region were examined and complete realization of the vortices was demonstrated to be necessary for accurate MFU turbulence statistics requiring a minimum spanwise domain length $L_{\mathrm{z}} = \pi$. For the neutrally stratified Ekman layer, the higher-order moments of velocity were examined and the accuracy of a kurtosis model was assessed. For the unstable Ekman layer, the analysis of higher-order moments was extended to temperature-velocity correlations. Model coefficients were optimised using DNS data and it was shown that the optimised models accurately captured the distributions of all fourth-order moments. These flow fields represent complex turbulence which will be subject to flow and heat transfer control by phonons at a later stage of our work. Research aimed at the control of fully turbulent channel flow using direct numerical simulation (DNS) was also conducted. The reduction of the kinetic energy of large amplitude perturbations in channel flow was investigated using passive phononic (periodic) structures. These studies, and the results obtained, lay the foundation for extending the phononic subsurface passive control methodology to turbulent drag in channel flows. Results from this seed grant have appeared in three journal articles and have been accepted for presentation at national conferences.

I. RESEARCH

Several different research endeavors were conducted, all involving the integration of the time-dependent Navier-Stokes equations using direct numerical simulation (DNS).

A. Spanwise-Rotating Turbulent Channel Flow and Modeling

Turbulent channel flow subject to rotation in the spanwise direction is characterized by reduced turbulence levels near one wall and elevated turbulence levels near the opposite wall; these regions are known as the suction and pressure sides, respectively[1]. Subsequently, the symmetric profiles of mean velocity and Reynolds stress distributions in the non-rotating channel become asymmetric with respect to the channel centerline. The effects of spanwise rotation on momentum transport in turbulent channel flow has been well documented in previous direct numerical simulation (DNS) studies by Grundestam et al.[1] and Wu and Kasagi[2]. Rotation-induced body forces (Coriolis, centrifugal) generate a secondary cross flow, and consequently a particular type of complex turbulent flow regime is developed with more than one mean flow gradient. The analyses of such complexities on the structure and parameterization of turbulence have relevance to engineering applications such as gas turbine blade and rotating turbomachinery design, especially with regards to surface heat transfer and skin friction within the internal cooling passages[3,4].

For the research conducted and published in Hsieh, Biringen, and Kucala[5], DNS was employed to assess four RANS models proposed by (a) Reif et al.[6] (PRDO), (b) Speziale and Gatski[7] (SG), (c) Girimaji[8] (GI) and (d) Grundestam et al.[9] (GWJ). Two algebraic heat flux models proposed by (e) Younis et al.[10] (YWL) and (f) Abe and Suga[11] (SA) were also evaluated. In addition, the pressure-strain functions proposed in Speziale and Gatski[7] and Girimaji[8] were investigated for their influence on the modeled Reynolds stress distributions.

For spanwise-rotating turbulent channel flow, the Reynolds stress distributions produced from a linear and nonlinear eddy viscosity model were compared to demonstrate improved accuracy for the nonlinear model over the linear model. In a comparison of four nonlinear eddy viscosity models with DNS data, EARSM were the most compatible with DNS results in modeling the Reynolds stresses for turbulent channel flow subject to spanwise rotation. The Speziale-Gatski model was shown to be the most compatible for zero and low rotation numbers but displayed significant deviations near the pressure wall at high rotation numbers. As shown in figure 1, the Grundestam-Wallin-Johansson model showed the best agreement with the DNS data at high rotation numbers. Heat flux models were in good agreement with DNS data for the no-rotation case but with system rotation, the models deviated from the DNS, increasing at higher rotation rates.

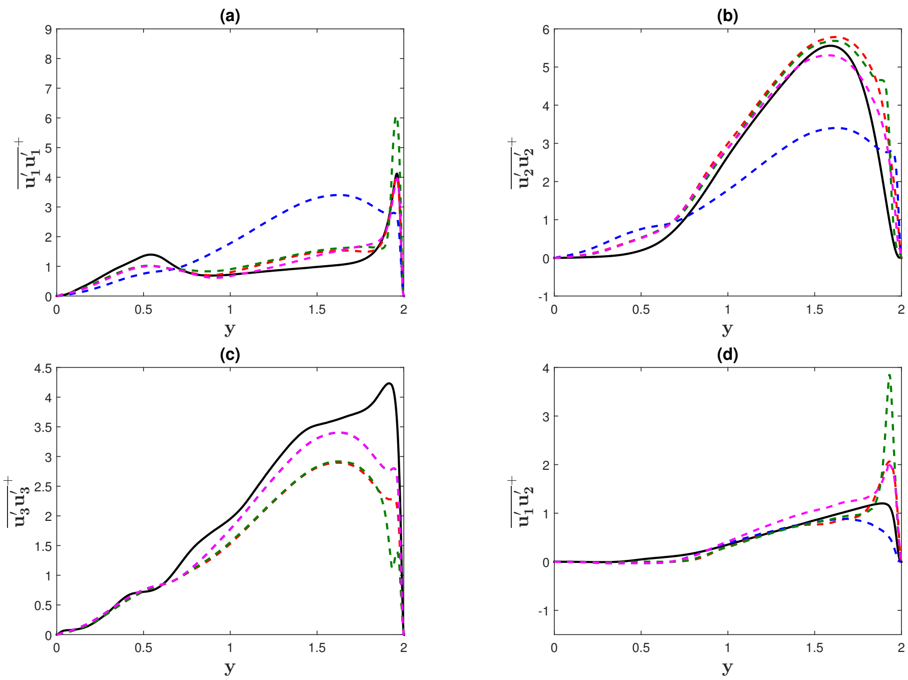

FIG. 1: Modeled Reynolds stress profiles for $Ro_\mathrm{b} = 0.9$. (a) $\overline{u_1'u_1'}^+$; (b) $\overline{u_2'u_2'}^+$; (c) $\overline{u_3'u_3'}^+$; (d) $\overline{u_1'u_2'}^+$. Black: DNS; blue: PRDO; green: SG; red: GI; magenta: GWJ.

The pressure-strain models of two EARSM (Girimaji, SG) were shown to have significant disagreements with the DNS data in the near-wall regions and the pressure-temperature-gradient models of two EAHFM (YWL, SA) demonstrated inaccurate characterization of the suction region with system rotation. The errors in the modeled contributions from these terms resulted in degeneration of the predictive capabilities of their respective closure models. These errors contributed to inaccurate Reynolds stress amplitudes in the near-wall regions and an inaccurate modeled distribution shape for wall-normal turbulent heat flux in EARSM and EAHFM, respectively. Present results indicate correct characterization of pressure fluctuations is a crucial factor in both EARSM and EAHFM design for spanwise-

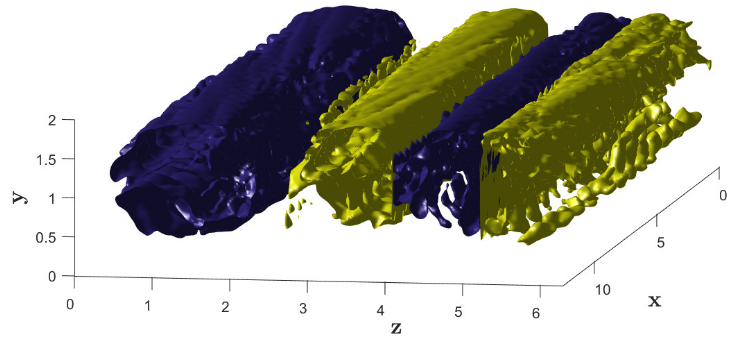

FIG. 2: Three-dimensional contours of time-averaged v and w velocity for $Ro_{\mathrm{b}} = 0.5$. Dark and light contours denote clockwise and counter-clockwise motion, respectively.

rotating turbulent channel flow.

B. Spanwise-Rotating Turbulent Channel Flow and the Minimal Flow Unit

For spanwise-rotating turbulent channel flow, the streaky and vortical structures associated with the turbulence sustenance cycle[12,13] persist in the pressure region and the generation of additional turbulence structures was observed in the rotational turbulence studies of Kristofferson and Andersson[14] and Grundestam *et al.*[1]. In figure 2, one example of the rotation-induced flow instabilities, known as roll cells, are shown to circulate flow throughout the pressure region of the chnnel.

In order to determine the dimensions of a minimal flow unit, it is imperative to examine the contributions of these rotation-induced structures to turbulence. The concept of the minimal flow unit (MFU) model is based on the determination of the smallest computational box size that will produce acceptably accurate turbulence statistics at minimal computational cost. As the dependence of turbulence production on the interactions of various turbulence structures has been well documented in literature[13,15], MFU design distinguishes a basic set of structures necessary to sustain turbulence and constructs a shorter domain based on this array of structures. A model's success is determined by its ability to accurately predict essential turbulence statistical quantities at a significantly reduced computational cost com-

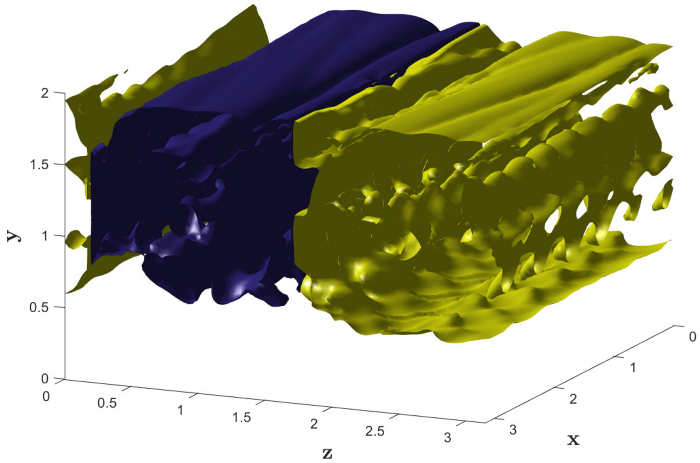

FIG. 3: Three-dimensional contours of time-averaged v and w velocity for MFU simulation case at $Ro_{\mathrm{b}} = 0.5$. Dark and light contours denote clockwise and counter-clockwise motion, respectively.

pared to full direct numerical simulation (DNS) on a well-resolved computational domain. Such MFU models are necessary for computational fluid dynamics research requiring large amounts of simulations such as parametric studies for flow control[16,17]. For the research conducted and published in Hsieh and Biringen[18], the DNS database for turbulent channel flow, subject to varying rotation and Reynolds numbers, was used to assess the accuracy of the MFU model for predicting low and high-order moments of turbulent fluctuations.

For the design of a minimal flow unit for rotational turbulence, a baseline MFU model with spanwise domain length of $L_z = \pi\delta$ was selected to accomodate a single full pair of Taylor-Gortler vortices as shown in figure 3. A box minimization study with reduced spanwise domain lengths down to $L_z = 0.18\pi\delta$, the MFU length for the non-rotating turbulent channel flow, was conducted. Observed discrepancies in the mean velocity distributions demonstrated that MFU accuracy did not depend on sublayer streak distance as for the non-rotational channel and a significantly larger minimum spanwise length $L_z = \pi\delta$ was required for accurate turbulent statistics, corresponding to the minimum length for proper realization of one full pair of Taylor-Gortler vortices. If these vortices were inaccurately represented from further truncation of the spanwise domain length, turbulent fluctuations were inaccurate or an incorrect mean velocity gradient was produced in the pressure region.

For a higher-Reynolds number, the MFU model demonstrated decreased accuracy compared to the low-Reynolds simulation. Hence for large Reynolds numbers, MFU models may require a significantly larger domain box to accurately approximate turbulence statistics and alternative factors for MFU design require consideration, such as Reynolds number effects on sublayer streak length and turbulence structures in the suction region. To test the limitations of the MFU model, higher-order statistics from the baseline MFU model were compared to those from the full simulations. The model produced accurate distributions of skewness and kurtosis for a non-rotating channel but was unable to maintain this accuracy with rotation in the suction region. The MFU model accurately captured higher-order statistics in the pressure region due to the successful realization of roll cells but could not properly capture the re-laminarized suction region which contained intermittent high-amplitude velocity fluctuations, a consequence of the turbulent spots structures. These findings indicated that when the MFU model was extended beyond its intended function of general turbulence quantities (mean velocity, Reynolds stresses) to higher-order statistics, the model continued to perform well in regions of high turbulence due to its ability to capture the coherent structures which contribute to turbulence production. However, the model failed in regions with different physical dynamics such as the low-turbulence suction region.

C. Ekman Layer Flow and Modeling

The Ekman layer[19] is a boundary layer formed by pressure gradients in a rotating system[20]. With a heated surface (convective boundary layer) and capped inversion, the Ekman layer is often used to model the complex dynamics of the atmospheric boundary layer (ABL) such as buoyant forcing and effects of Coriolis forces due to the Earth's rotation[21,22]. Similar to the turbulent channel problem, turbulence closure models that consider time-averaged equations with phenomenological closure approximations are highly desirable if they can accurately parameterise turbulent transport.

For the research conducted and published in Waggy, Hsieh, and Biringen[23], the DNS database under both neutral and unstable conditions was utilized to assess closure models used for predicting high-order moments of turbulence and temperature fluctuations as a function of lower-order correlations. The higher-order moments of skewness and kurtosis in the turbulent Ekman layer were examined; an assessment of a model proposed by Mole and Clarke[24] for the kurtosis was also provided. For the unstable Ekman layer, analysis of higher-order moments was extended to temperature-velocity correlations, and two closure models by Zilitinkevich *et al.*[25] and Gryanik and Hartmann[26] were evaluated.

Evaluation of the DNS results with previous similar studies[27,28] showed strong agreement, lending validity to the simulation results used for turbulence modeling. The higher-order moments of skewness and kurtosis were introduced in the case of a neutrally stratified Ekman boundary layer and a model proposed by Mole and Clarke[24] for the kurtosis was evaluated. An analysis of two separate sets of coefficients proposed for the model by Tampieri *et al.*[29] and Alberghi *et al.*[30] demonstrated that the coefficients proposed by Alberghi *et al.*[30] generally had better agreement with the DNS data. In the case of an unstratified Ekman boundary layer, two closure models by Zilitinkevich *et al.*[25] and Gryanik and Hartmann[26] approximated third and fourth-order moments of velocity and temperature as a function of lower order moments as well as the skewness and kurtosis. A parametric study using the explained variance (σ_f^2) was conducted to assess the accuracy of the coefficients proposed by each of these models and propose a new set of coefficients that would maximise σ_f^2. The computed model coefficients that maximised σ_f^2 did well in accurately capturing the trend of all fourth-order moments as well as some third-order moments.

D. Flow Control: Channel Flow

Flow control in regards to jet turbines has been a subject of great interest in recent years. Turbulence is an impediment to effective turbine design due to its flow regime consisting of chaotic property changes and instabilities, leading to undesirable results such as higher drag and energy losses[31]. Flow control is also a major topic of research for friction drag reduction which too is directly connected to instabilities[32]. Flow control focuses on the reduction of these instabilities using active (non-zero energy cost) or passive (zero energy cost) methods. This research examined passive flow control using phononic crystals placed underneath the surface. A phononic crystal is a periodic material formed by the repeated spatial arrangement of a unit cell[33,34]. The unit cell exhibits a band structure that relates the frequency to the wavenumber of elastic waves traveling across the phononic crystal as a whole. Among the features of a band structure that is widely used in phononic-crystal

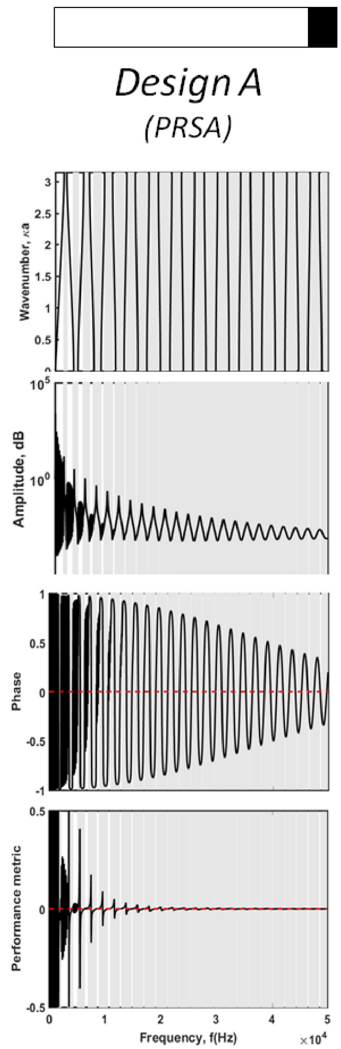

FIG. 4: Wavenumber, amplitude, phase and performance metric curves vs. frequency for a phononic subsurface design labeled Design A.

applications is the presence of band gaps (frequency ranges were waves are prohibited from propagation[35]. In the context of flow control, our previous research has demonstrated that within a stop band, not only the waves are prohibited from propagation, but their phase changes in a robust manner, i.e., independent of the boundary conditions. When combining this effect to the tuning of the finite phononic crystal resonance response, we have shown that it is possible to use this mechanism for passive stabilization of a laminar flow exhibiting a growing Tollmien-Schlichting (TS) instability[17].

As shown in figure 4, the effect of a particular phononic subsurface design over a large frequency range varies significantly depending on the layering of individual materials within

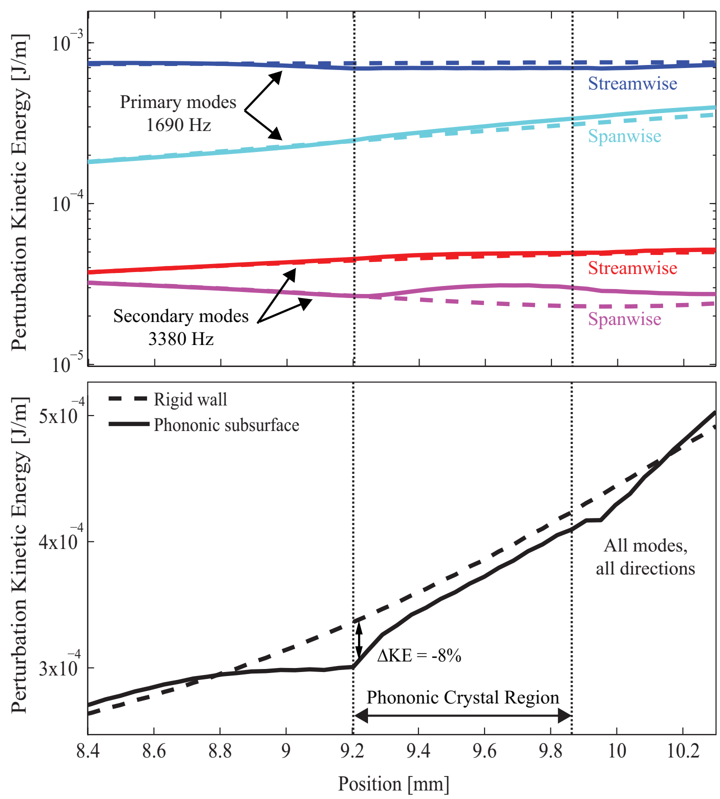

FIG. 5: Streamwise spatial distributions of the kinetic energy of the disturbance field within the bottom half of the channel; the dotted lines represents the base model (i.e., with no control) and the continuous lines represent the model with the phononic crystal. The plotted quantity represents the spatial intensity of the flow instability.

the unit cell. Despite the material system as a whole being composed of only two constituent materials (ABS polymer and aluminum), the number of layers as well as the volume fraction of each constituent material may be modified freely. Hence optimization studies can be performed to tuning these phononic subsurfaces to suppress the turbulence mechanisms. Our research aims to produce an optimized phononic subsurface structure which significantly reduces both turbulent kinetic energy and drag in turbulent channel flow.

Prior to investigating the turbulence problem, it is important to examine the effects of large amplitude disturbances since these bring rise to nonlinear effects. To examine the ability of a phononic subsurface to counter large-amplitude instabilities, we conducted coupled fluid-structure direct numerical simulations where we introduced an initial excitation wave incorporated as a spatially evolving disturbance in a fully-developed plane Poiseuille (channel) flow driven by a mean pressure gradient. The channel is formed by parallel walls at the bottom and at the top with periodic boundary conditions applied in the spanwise z-direction, and a buffer (sponge) layer is used to model the outflow. In the fluid part of the coupled model, the base flow is an exact solution of the Navier-Stokes equation. We superimposed an unstable spatial solution (eigenfunction) of the Orr-Sommerfeld equation at the inflow boundary of the channel to excite the parabolic base velocity, faithfully modeling the conditions in typical laboratory experiments. We consider water as the working fluid, a Reynolds number Re = 7500, and a non-dimensional unstable frequency $\omega_R = 0.25$ (i.e. 1690Hz). In the solid domain, the Newmark scheme was used for the time integration. The unit cell of the phononic crystal configuration considered was again composed of aluminum and ABS polymer. The density, ρ_s and Youngs modulus, E_s, for each of these two constituent materials are: $\rho_{Al} = 2700$ Kg/m3, $\rho_{ABS} = 1040$ Kg/m3, $E_{Al} = 68.8$ GPa, $E_{ABS} = 2.4$ GPa. Both the structure and the fluid equations are inverted separately and a conventional serial staggered approach is used to couple the interface between the two.

The streamwise evolution of selected modal contributions of perturbation kinetic energy (KE) is shown in Fig. 5(a). Compared to the reference all-rigid-wall case (dashed lines), it is observed that the perturbation KE decreases across the length of the phononic crystal interface for the primary mode (blue). However, this effect is reversed for the three other modes presented and may be explained by nonlinear interactions. This reversed effect is somewhat negligible, however, owing to the difference in the orders of magnitude of the modal energies. By only stabilizing the primary mode, we show a reduction of maximum 8% in the total perturbation kinetic energy (summed over all modes) as shown in Fig. 5(b). These results demonstrate the ability of the phononic crystal to stabilize the three-dimensional flow field [the type exhibited by flows undergoing secondary (K-type) transition] via frequency-dependent wave interferences, even in the presence of large-amplitude, nonlinear disturbances.

II. COMPUTATIONAL METHOD

Direct simulations are important to the scientific community because of the detail they offer into the dynamics of a flow. Near boundaries a fine mesh is required to capture the smallest scales of turbulent motion. In many instances, DNS allows monitoring of

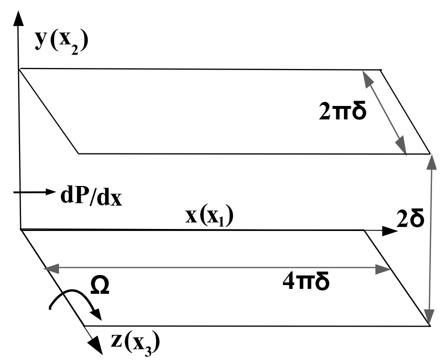

FIG. 6: Diagram of turbulent channel flow with rotation in the spanwise direction.

flow variables closer to the wall than experimentation. DNS is the ideal tool to use in problems dealing with flow control, where very precise calculation of the near-wall dynamics is critical. Other methods, such as Reynolds Averaged Navier-Stokes (RANS) and large-eddy simulations (LES), while able to capture the large scales in the problem, are unable to resolve smaller scales of turbulence. The use of DNS bypasses this problem, but at a much higher cost of computational resources.

A. Numerical Algorithm and Parallel Architecture

For the problems described above, we incorporate a semi-implicit finite difference method to solve the incompressible Navier-Stokes (N-S) equations. The nonlinear advective terms are solved using a second-order time and fourth-order spatial variant of the Adams-Bashforth explicit time integrator. Diffusive terms are solved using a variant of the implicit Crank-Nicholson method (also second-order in time and fourth-order space). A corrector step is then applied to the predictor velocities to enforce zero divergence at the new time step. This operation requires solving a Laplaces equation, at each time step. In summary, advancing a solution one time step requires solving four linear systems for the fractional step velocities and temperature and one Laplaces equation for the pseudo-pressure ϕ at the next time level.

The above algorithm was implemented using the PETSc libraries. Storage savings are incorporated by only allocating storage for locally owned data on each process and the ghost points from adjacent processes. Similarly, coefficients of linear systems are only saved for local grid points. A sparse storage technique has been implemented to speed up computation the solution of linear systems and save storage.

The solution of the fractional step velocities and temperature field converge quickly using the PETSc provided GMRES Krylov subspace solver. However, solving for the pseudo-pressure involves a much stiffer system due to the full Neumann boundary conditions necessary at the rigid boundaries of the domain for the incompressible N-S equations. The singularity of the system is addressed by removing the null space from the solution.

Two main versions of the code were created: a doubly-periodic channel code with periodic boundary conditions in the streamwise and spanwise directions, and a streamwise spatial code with a periodic spanwise direction. The spatial code was modified for an Ekman layer or channel through a simple adjustment of the boundary conditions.

III. SUMMARY

The objective of this research was to investigate in detail the dynamics of turbulence in simple and complex turbulent flows, primarily with regards to understanding the contributions of coherent structures to the turbulence generation cycle and the ability of closure models to accurately approximate turbulence. In ascertaining the interactions and roles of energetical structures as well as their relationships with intercomponent energy transfer and overall turbulent kinetic energy, the underlying complex mechanisms behind turbulence are now better understood. The examination of turbulence and heat transfer closures also assisted this objective as in addition to attaining significant reductions of computational costs, the understanding of intercomponent energy transfer and turbulence production is crucial within model design and improvement. In parallel, we have applied passive flow control by phononic subsurfaces on three-dimensional disturbances, exhibited by flows undergoing secondary (K-type) transition, and demonstrated that this concept is successful even for large-amplitude nonlinear instabilities. The next step in the research is to combine the two thrusts and design phononic-crystal structures tuned for turbulent flow in order to realize systemic suppression of targeted coherent structures.

The publications referenced in Refs. [5], [18], and [23] have been direclty funded by this research.

---

* mih@colorado.edu

[†] Sedat.Biringen@colorado.edu

[1] O. Grundestam, S. Wallin, and A. Johansson, J. Fluid Mech. **598**, 177 (2008).

[2] H. Wu and N. Kasagi, Phys. Fluids **16**, 979 (2004).

[3] S. Acharya, E. Sethuraman, and S. Nikotopoulos, J. Turbomachinery **131**, 1 (2012).

[4] D. Lakehal, J. Turbomachinery **124**, 485 (2002).

[5] A. Hsieh, S. Biringen, and A. Kucala, J. Turbomach. **138**, 1 (2016).

[6] B. P. Reif, P. Durbin, and A. Ooi, Int. J. Heat Fluid Flow **20**, 563 (1999).

[7] C. Speziale and T. Gatski, J. Fluid Mech. **254**, 59 (1993).

[8] S. Girimaji, Theo. Comp. Fluid Mech. **8**, 387 (1996).

[9] O. Grundestam, S. Wallin, and A. Johansson, Int. J. Heat and Fluid Flow **26**, 732 (2005).

[10] B. Younis, B. Weigand, and A. Laqua, J. Heat Transfer **134**, 1 (2012).

[11] K. Abe and K. Suga, Int. J. Heat and Fluid Flow **22**, 19 (2000).

[12] J. Kim, P. Moin, and R. Moser, J. Fluid Mech. **177**, 133 (1987).

[13] M. Landahl, J. Fluid Mech. **212**, 593 (1990).

[14] R. Kristofferson and H. Andersson, J. Fluid Mech. **253**, 163 (1993).

[15] W. Schoppa and F. Hussein, J. Fluid Mech. **453**, 57 (2002).

[16] A. Kucala and S. Biringen, J. Fluid Mech. **738**, 105 (2014).

[17] M. I. Hussein, S. Biringen, O. R. Bilal, and A. Kucala, Proc. R. Soc. A **471**, 20140928 (2015).

[18] A. Hsieh and S. Biringen, Phys. Fluids **12**, 125102 (2016).

[19] V. W. Ekman, Arch. Math. Astron. Phys. **2**, 1 (1905).

[20] S. Marlatt, S. Waggy, and S. Biringen, J. Atm. Sci. **69**, 1106 (2012).

[21] S. B. Waggy, S. Biringen, and P. P. Sullivan, J. Fluid Mech. **724**, 581 (2013).

[22] S. Waggy, S. Biringen, and A. Kucala, Geophysical and Astrophysical Fluid Dynamics **109**, 465 (2015).

[23] S. Waggy, A. Hsieh, and S. Biringen, Geophys. Astrophys. Fluid Dynamics **110**, 391 (2016).

[24] N. Mole and E. D. Clarke, Bound. Layer Meteor. **73**, 35 (1995).

[25] S. S. Zilitinkevich, V. M. Gryanik, V. N. Lykossov, and D. V. Mironov, J. of Atm. Sci. **56**, 3463 (1999).

[26] V. M. Gryanik and J. Hartmann, J. of Atm. Sci. **59**, 2729 (2002).

[27] P. R. Spalart, G. N. Coleman, and R. Johnstone, Phys. Fluids **20** (2008).

[28] K. Miyashita, K. Iwamoto, and H. Kawamura, Journal of the Earth Simulator **6**, 3 (2006).

[29] F. Tampieri, A. Maurizi, and S. Alberghi, in *Ingegneria del Vento in Italia 2000*, edited by G. Solari, L. C. Pagnini, , and G. Piccardo (S.G.E., Valenzuela City, Metro Manila, 2000) pp. 37–50.

[30] S. Alberghi, A. Maurizi, and F. Tampieri, J. of Applied Meteorology **4**, 885 (2002).

[31] D. Rizzetta and M. Visbal, J. Fluids Engineering **128**, 956 (2006).

[32] M. Gad-el Hak, Progress in Aerospace Sciences **38**, 77 (2002).

[33] M. I. Hussein, G. M. Hulbert, and R. A. Scott, Journal of Sound and Vibration **289**, 779 (2006).

[34] M. I. Hussein, G. M. Hulbert, and R. A. Scott, Journal of Sound and Vibration **307**, 865 (2007).

[35] M. I. Hussein, M. J. Leamy, and M. Ruzzene, Appl. Mech. Rev. **66**, 040802 (2014).

AFOSR Deliverables Submission Survey

Response ID:7677 Data

1.

Report Type

Final Report

Primary Contact Email
Contact email if there is a problem with the report.

mih@colorado.edu

Primary Contact Phone Number
Contact phone number if there is a problem with the report

3034923177

Organization / Institution name

University of Colorado Boulder

Grant/Contract Title
The full title of the funded effort.

Phononic Subsurface: A New Paradigm for Turbulence Control for Drag Reduction

Grant/Contract Number
AFOSR assigned control number. It must begin with "FA9550" or "F49620" or "FA2386".

FA9550-15-1-0495

Principal Investigator Name
The full name of the principal investigator on the grant or contract.

Mahmoud Hussein

Program Officer
The AFOSR Program Officer currently assigned to the award

Douglas R. Smith

Reporting Period Start Date

09/30/2015

Reporting Period End Date

09/29/2016

Abstract

Direct numerical simulations (DNS) of spanwise-rotating turbulent channel flow as well as the neutral and unstable turbulent Ekman layer were conducted. These DNS results were used to evaluate various turbulence and heat transfer models for the Reynolds stresses, turbulent heat fluxes and higher-order moments of velocity and temperature. Explicit Algebraic Reynolds Stress Models (EARSM) obtained the Reynolds stress distributions in best agreement with DNS data for rotational flows and turbulent heat flux distributions obtained from two explicit algebraic heat flux models consistently displayed increasing disagreement with DNS data with increasing rotation rate. DNS results were also used to determine the proper computational box size for a minimal flow unit (MFU) at Ro_b=0.5. For the neutrally stratified Ekman layer, the higher-order moments of velocity were examined and the accuracy of a kurtosis model was assessed. For the unstable Ekman layer, the analysis of higher-order moments was extended to temperature-velocity correlations. These flow fields represent complex turbulence

which will be subject to flow and heat transfer control by phonons at a later stage of our work. Research aimed at the control of fully turbulent channel flow using DNS was also conducted. The reduction of the kinetic energy of large amplitude perturbations in channel flow was investigated using passive phononic structures. These studies, and the results obtained, lay the foundation for extending the phononic subsurface control methodology to turbulent drag in channel flows. Results from this seed grant have appeared in three journal articles and have been accepted for presentation at national conferences.

Distribution Statement

This is block 12 on the SF298 form.

Distribution A - Approved for Public Release

Explanation for Distribution Statement

If this is not approved for public release, please provide a short explanation. E.g., contains proprietary information.

SF298 Form

Please attach your SF298 form. A blank SF298 can be found here. Please do not password protect or secure the PDF The maximum file size for an SF298 is 50MB.

FA9550-15-1-0495_SF_298_Submitted_02.27.2017.pdf

Upload the Report Document. File must be a PDF. Please do not password protect or secure the PDF . The maximum file size for the Report Document is 50MB.

2017_AFOSR_Final_Report_Feb_2017.pdf

Upload a Report Document, if any. The maximum file size for the Report Document is 50MB.

Archival Publications (published) during reporting period:

Please final report document.

New discoveries, inventions, or patent disclosures:

Do you have any discoveries, inventions, or patent disclosures to report for this period?

No

Please describe and include any notable dates

Do you plan to pursue a claim for personal or organizational intellectual property?

Changes in research objectives (if any):

N/A

Change in AFOSR Program Officer, if any:

N/A

Extensions granted or milestones slipped, if any:

N/A

AFOSR LRIR Number

LRIR Title

Reporting Period

Laboratory Task Manager

Program Officer

Research Objectives

Technical Summary

Funding Summary by Cost Category (by FY, $K)

	Starting FY	FY+1	FY+2
Salary			
Equipment/Facilities			
Supplies			
Total			

Report Document

Report Document - Text Analysis

Report Document - Text Analysis

Appendix Documents

2. Thank You

E-mail user

Feb 27, 2017 15:23:25 Success: Email Sent to: mih@colorado.edu